Ab initio investigation of electron paramagnetic resonance parameters of S_2^-, SSe^-, and Se_2^- radicals in alkali halides

F. Stevens,[1,2] H. Vrielinck,[1] F. Callens,[1,*] E. Pauwels,[2] and M. Waroquier[2]
[1]*Ghent University, Department of Solid State Sciences, Krijgslaan 281-S1, B-9000 Ghent, Belgium*
[2]*Ghent University, Laboratory of Theoretical Physics, Proeftuinstraat 86, B-9000 Ghent, Belgium*
(Received 22 October 2002; published 31 March 2003)

Density functional theory (DFT) methods, as implemented in the Amsterdam Density Functional program, are used to calculate the electron paramagnetic resonance (EPR) and electron nuclear double resonance (ENDOR) parameters of S_2^-, SSe^-, and Se_2^- molecular ions doped into NaZ (Z=Cl,Br,I) and KI lattices. The calculations are performed on cluster in vacuo models, involving 88 atoms for the defect and its lattice surroundings, assuming that the molecular anions replace a single halide ion. In a previous study on the S_2^- ion, difficulties were encountered in calculating the superhyperfine and quadrupole principal values and axes of the neighbor cation nuclei. The observed discrepancies were partially attributed to the use of the frozen core approximation. In this work, the influence of this approximation on the calculated EPR and ENDOR parameters is evaluated. The DFT results for the S_2^-, SSe^-, and Se_2^- molecular ions are in good agreement with the available experimental EPR data for all considered lattices, strongly supporting the monovacancy model for these diatomic defects.

DOI: 10.1103/PhysRevB.67.104429 PACS number(s): 76.30.Mi

I. INTRODUCTION

In a previous study, electron paramagnetic resonance (EPR) and electron nuclear double resonance (ENDOR) parameters of the S_2^- molecular ion doped in various alkali halide lattices were studied theoretically,[1] using density functional theory (DFT) methods. Herein, the main issue was the search for an accurate description of the paramagnetic defect and its lattice surroundings. It was found that a cluster in *vacuo* containing 88 atoms could satisfactorily reproduce all experimental EPR parameters (g and the hyperfine tensor of the central molecular ion), if relaxations of the first two lattice shells were considered. In spite of these computational successes, large discrepancies were encountered between calculated and experimental principal superhyperfine and quadrupole values and axes for the nearest neighboring cation nuclei.

In order to improve the calculated superhyperfine and quadrupole tensors, we will investigate the influence of the frozen core approximation on these parameters by gradually unfreezing the used cluster, i.e., by removing the frozen core approximation of subsequent lattice shells. A partially unfrozen cluster is used because a fully unfrozen cluster is computationally not feasible. Such calculations are performed on the S_2^- molecular ion doped in NaCl, and the results are compared to those of our previous study.[1] Once the most adequate partially unfrozen cluster is found, these calculations are extended to the S_2^-, Se_2^-, and SSe^- molecular ions in NaZ (Z = Cl, Br, I) and KI lattices, for which experimental EPR and ENDOR data are also available.[2–10] By comparison with experiment, we shall investigate the level of accuracy that can be expected, within the applied approximations, in calculating EPR and ENDOR parameters of these paramagnetic diatomic chalcogen defects. In all our calculations a monovacancy model is used, in which the diatomic molecular ion replaces one halide ion in the alkali halide lattice (see Fig. 1) and the intramolecular axis is oriented along a $\langle 110 \rangle$ direction.

The structure of the present paper is as follows. In Sec. II, a short discussion of the spin Hamiltonian parameters used in the analysis of the XY^- and X_2^- (X, Y=S, Se) molecular ions is given. The computational details are summarized in Sec. III. In Sec. IV, the influence of the frozen core approximation is evaluated for the system NaCl:S_2^- and the DFT results for S_2^-, SSe^-, and Se_2^- in the aforementioned alkali

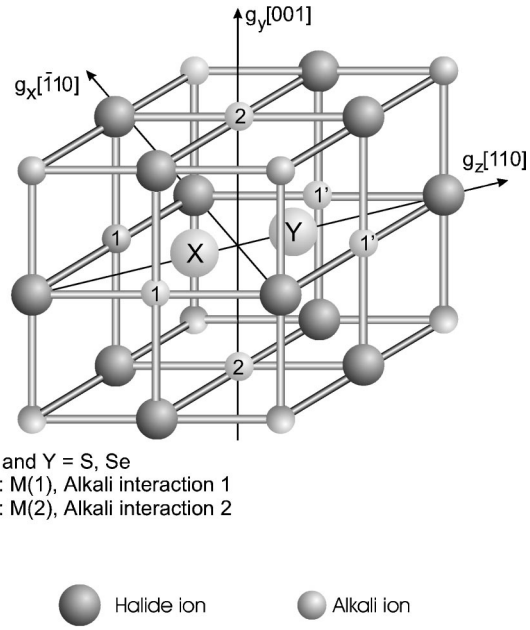

FIG. 1. The XY^- ion in alkali halides, assuming a monovacancy model (X,Y=S or Se). For SSe^-, the 1 and 1′ nuclei are inequivalent.

halide lattices are compared with experiment. The main conclusions are given in Sec. V.

II. THEORY OF EPR AND ENDOR PARAMETERS

The free X_2^- and XY^- molecular ions have $D_{\infty h}$ and $C_{\infty v}$ symmetries and a $(2\pi_g)^3$ and $(2\pi)^3$ electron configuration, respectively. In the alkali halide crystal lattice, the symmetry is lowered to D_{2h} and C_{2v}. The degeneracy of the π_g and π orbitals is lifted and either a $^2B_{2g}$ or $^2B_{3g}$ ground state results for the X_2^- molecular ions. For the XY^- molecular ions, the corresponding possibilities are $^2B_1$ and $^2B_2$ (also see below).[11]

In all cases, the paramagnetic defect has $S=\frac{1}{2}$ and can be described by a spin Hamiltonian[12]

$$\hat{H}_S=\mu_B\vec{B}\overline{g}\hat{\vec{S}}-\sum_i g_{N,i}\vec{B}\hat{\vec{I}}_i+\sum_i \hat{\vec{S}}\overline{A}_i\hat{\vec{I}}_i+\sum_i \hat{\vec{I}}_i\overline{Q}_i\hat{\vec{I}}_i. \quad (1)$$

The first term in this equation is the electronic Zeeman term, which describes the interaction between the electron spin $\vec{S}$ and the external magnetic field $\vec{B}$, and is parametrized by the g tensor.

The second term is the nuclear Zeeman term, which describes the interaction between the applied magnetic field $\vec{B}$ and a nuclear spin $\vec{I}_i$. This interaction is parametrized by the nuclear g tensor $\overline{g}_{N,i}$, which in most cases reduces to a scalar $g_{N,i}$.

If the nucleus i belongs to the central X_2^- or XY^- molecular ion, the interaction $\hat{\vec{S}}\overline{A}_i\hat{\vec{I}}_i$ will be called a hyperfine interaction. Interactions with neighboring nuclei will be referred to as superhyperfine interactions.

The last term in the spin Hamiltonian is the nuclear quadrupole interaction parametrized by the quadrupole tensor Q_i $(I_i>\frac{1}{2})$. To first order, the EPR spectrum gives no information about this interaction. The quadrupole tensor describes the interaction between the electric quadrupole moment of the nucleus and electric field gradients, which are present.

Symmetry requires that the g tensor is rhombic $(g_x\neq g_y\neq g_z\neq g_x)$ and that the principal axes are oriented along $[110]$ (g_z), $[\bar{1}10]$ (g_x) and $[001]$ (g_y), or equivalent conformations (Fig. 1). According to the theory of Refs. 13–15 (X_2^- molecular ions) and Ref. 8 (XY^- molecular ions), the g tensor is characterized by $g_x<g_y<g_z$ if the molecular ion has the $^2B_{2g}$ or $^2B_1$ ground state and by $g_y<g_x<g_z$ in case of the $^2B_{3g}$ or $^2B_2$ ground state. The smallest g value is found along the direction of the paramagnetic p lobes of the molecular ion. Because inversion symmetry is lost for the XY^- molecular ions, certain ions of a particular lattice shell become inequivalent. This is illustrated in Fig. 2(a), for the interaction with the four nearest cation neighbors in the g_x-g_z plane, defined as interaction 1. Whereas for the X_2^- defect, all four ions are equivalent, in the case of the XY^- defect, the ions labeled 1 and $1'$ are no longer equivalent. We will denote the A and Q tensor properties of the ions closest to Se with accents. The loss of inversion symmetry may also cause additional tiltings of principal axes. Indeed, for the XY^- molecular ions, symmetry allows the A and Q tensor axes of interaction 2 to be tilted away from the g tensor axes, by the angle β_A and β_Q, as illustrated in Fig. 2(b).

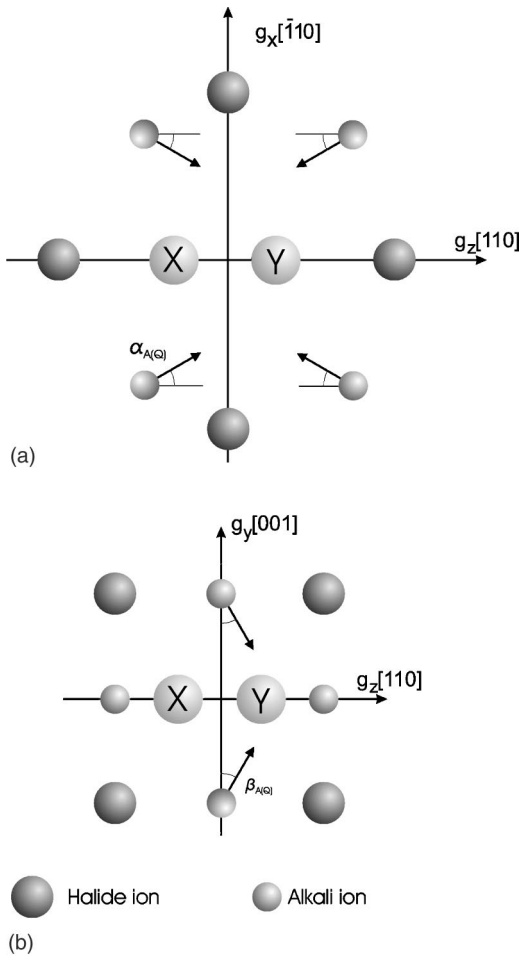

FIG. 2. The applied nomenclature for the different superhyperfine interactions. The tilting angle in the g_z-g_x plane, between the $A_z(Q_z)$ and g_z principal axes is defined as $\alpha_A(\alpha_Q)$. For the SSe^- defect, the angle between the $A_y(Q_y)$ and g_y principal axes is defined as $\beta_A(\beta_Q)$.

III. COMPUTATIONAL DETAILS

All geometry optimizations and EPR calculations are based on DFT (Refs. 16–18) principles and were performed with the Amsterdam density functional (ADF) program package, version 1999.[19–21] This program comprises a set of routines to evaluate the g, A, and Q tensors as developed and implemented by van Lenthe and co-workers.[22–24]

Standard basis set IV was used,[25] employing Slater-type orbital basis functions. This set corresponds roughly to a triple-ζ basis set extended with polarization functions for main group elements. Calculations were performed adopting the local density approximation according to Vosko, Wilk, and Nusair's[26] parametrization of electron-gas data.

Within the concept of the full frozen core approximation, the following assumptions were made. For S, Cl, and Na, electrons up to the $2p$ shell were kept frozen. For Br and Se, electrons up to the $3d$ shell are frozen, while for I and K,

TABLE I. Influence of the frozen core approximation on EPR and ENDOR values of the S_2^- molecular ion doped in NaCl.

		frozen core			
			restricted		
	exp[a]	full[b]	S_2^- ion	shell 1	shell 2	shell 3
g_x	2.0107	2.0069	1.9902	2.0094	2.0096	2.0089
g_y	1.986	1.9837	1.967	1.9865	1.9868	1.986
g_z	2.2531	2.2343	2.3568	2.2642	2.2648	2.2686
A_x	$<A_y$	−28.5	−27.7	−30	−30	−29.9
A_y	108.5	67.4	69.5	71.4	71.3	71.3
A_z	$<A_y$	−10.3	−13.9	−10	−10.1	−9.7
$A_{x1,\mathrm{aniso}}$	0.57	1.04	1.05	0.85	0.85	0.84
$A_{y1,\mathrm{aniso}}$	0	−0.56	−0.63	−0.09	−0.09	−0.08
$A_{z1,\mathrm{aniso}}$	−0.57	−0.48	−0.42	−0.76	−0.76	−0.76
A_{iso}	3.91	−0.09	−0.15	−0.28	−0.29	−0.29
α_A	54.8	9.8	9.3	25.9	25.9	26.4
Q_{x1}	−0.53	−0.22	−0.22	−0.52	−0.53	−0.53
Q_{y1}	0.23	0.1	0.1	0.21	0.22	0.21
Q_{z1}	0.3	0.12	0.12	0.31	0.31	0.32
α_Q	−35.9	−32.1	−32.1	−32.1	−32.8	−32.9
$A_{x2,\mathrm{aniso}}$	−0.94	−0.94	−0.9	−1.06	−1.07	−1.08
$A_{y2,\mathrm{aniso}}$	0.36	1.03	1.01	0.79	0.79	0.79
$A_{z2,\mathrm{aniso}}$	0.58	−0.09	−0.1	0.28	0.28	0.29
A_{iso}	−4.41	−0.02	−0.03	−0.02	−0.02	−0.02
Q_{x2}	0.003	−0.004	−0.004	0.004	0.004	0.004
Q_{y2}	−0.007	0.023	0.023	−0.01	−0.01	−0.01
Q_{z2}	0.004	−0.019	−0.019	0.006	0.006	0.006

[a]Reference 4.
[b]Reference 1.

electrons up to the $4d$ and $3p$ shell were included in the core.

Within the zero-order regular approximation[27–33] for relativistic effects, all calculations were performed at the spin orbit spin unrestricted level of theory. The relativistic atomic potentials were calculated using the auxiliary program DIRAC,[34] as is comprised in the ADF program package.

IV. COMPUTATIONAL RESULTS

In our previous work,[1] geometry optimizations were performed on a cluster in vacuo containing 88 atoms. The chalcogen atoms, the nearest shell of M^+ (M = Na, K, Rb) and the next nearest shell of Z^- ions were allowed to relax. DFT-EPR calculations were subsequently performed on this optimized 88-atom cluster. In the present calculations, the same formalism is applied. The nomenclature for the different superhyperfine and quadrupole interactions is given in Fig. 2, as already discussed in Sec. II.

A. Influence of the frozen core approximation on EPR and ENDOR values of NaCl doped with S_2^-

The calculated EPR parameters for the S_2^- molecular ion doped in alkali halide lattices as performed in Ref. 1, were in good agreement with the experimental data, while the reproduction of the ENDOR parameters appeared to be more problematic. In order to search for an effective remedy to improve the experimental agreement, we released the frozen core restriction for a number of atoms in the cluster. The results for NaCl:S_2^- are presented in Table 1. We consider four classes in the restricted frozen core model. In the first class, the S_2^- ion is removed from the frozen core. In the second class (shell 1) all atoms included in the first lattice shell are released. In the two remaining classes, the number of ''unfrozen'' atoms is extended to the second and the third lattice shell respectively.

Releasing the frozen core approximation only for the S_2^- molecular ion, the discrepancy between calculated and experimental ^{33}S hyperfine values is partly removed, but the agreement for the g values becomes significantly worse. However, when the first shell cations are also considered unfrozen, the original agreement for the g values is restored and even slightly improved, while the ^{33}S hyperfine values remain unaffected. The unfreezing of further shells (second, third) does not seem to have a significant influence on the EPR and ENDOR parameters up to the first shell. Although a slight improvement of the calculated hyperfine values is obtained by removing the frozen core approximation, it does not appear to be the main cause for the discrepancy between

TABLE II. g tensor values for different diatomic lattice defects doped in NaZ (Z=Cl,Br,I) and KI. All theoretical values correspond with the partial frozen core approximation.

		Experimental			Theoretical		
		S_2^-	SSe^-	Se_2^-	S_2^-	SSe^-	Se_2^-
NaCl	g_x	2.0107[c]	1.9421[g]	1.8862[e]	2.0094	1.892	1.9141
	g_y	1.986	1.8818	1.7923	1.9865	1.8419	1.8226
	g_z	2.2531	2.6393	2.8356	2.2642	2.6812	2.7256
NaBr	g_x	2.0114[d]	1.9365[f]	1.9007[f]	2.0187	1.9359	1.9196
	g_y	1.9876	1.8916	1.8079	1.9935	1.8953	1.8407
	g_z	2.2379	2.6259	2.8073	2.2586	2.6229	2.7344
NaI	g_x	2.0178[b]	1.9675[a]	1.9042[a]	2.0189	1.9581	1.8795
	g_y	1.9942	1.9004	1.8148	2	1.9238	1.8211
	g_z	2.2303	2.6064	2.8015	2.2471	2.5943	2.8013
KI	g_x	1.6369[b]	0.9681[a]	0.7824[a]	1.5654	1.1042	0.7831
	g_y	1.6254	0.9532	0.7698	1.5537	1.0924	0.7752
	g_z	3.0629	3.629	3.7079	3.1655	3.5028	3.6229

[a]Reference 2.
[b]Reference 3.
[c]Reference 4.
[d]Reference 5.
[e]Reference 6.
[f]Reference 7.
[g]Reference 8.

the experimental and calculated values. In later work, we will explore the influence of the level of theory on these parameters.

Looking at the influence of the frozen core approximation on the ENDOR parameters of the neighboring nuclei, a significant improvement is noticed in reproducing the quadrupole tensors. For interaction 1, the agreement becomes impressive. Partially unfreezing the cluster also has a positive influence on the calculated hyperfine tensors, but the discrepancies with experiment cannot be completely removed. The tilting angle α_A was badly predicted in Ref. 1, a partial release of some atoms (shell 1) from the frozen core largely improves its value, but still not sufficiently.

Concluding we can state that a partial unfreezing of the considered 88-atom cluster yields a significant improvement of the ENDOR values but still some discrepancies remain. We can restrict ourselves to unfreezing the molecular ion and the first lattice shell, while the rest of the cluster can be kept frozen. This partial unfrozen cluster will be used in the following DFT-EPR calculations.

B. EPR parameters for NaZ and KI lattices

In Tables 2 and 3, calculated and experimental g and hyperfine values for the considered molecular ions doped in the aforementioned alkali halide lattices are listed. Within the monovacancy model, the correct ground state for all these MZ lattices is predicted, i.e., $^2B_{3g}$ for the S_2^- and Se_2^- molecular ions and $^2B_2$ for the SSe^- molecular ion.

1. S_2^- molecular ion

The calculated g and hyperfine values have the same qualitative agreement as in Ref. 1. When removing the full frozen core approximation, the quantitative agreement improves, especially the g and A values for the KI lattice.

2. SSe^- molecular ion

For the NaZ:SSe^- defects, the agreement between calculated and experimental g values is good. The observed trends in experimental g values when increasing the radius of the halide ion (g_y increases and g_z decreases) are reproduced by the calculations. Experimental hyperfine data are only available for the NaCl lattice. The experimental ^{77}Se interaction is much larger than the ^{33}S hyperfine interaction, which can partly be explained by comparing the corresponding magnetic moments ($g_{N,Se} \approx 2.5 g_{N,S}$). This behavior is perfectly reproduced by the calculations for the NaCl lattice. For the other NaZ lattices, the same qualitative results ($A_y > A_z > A_x$) as predicted for NaCl are found: the largest A value corresponds to the direction of the paramagnetic lobes.

The experimental g values for the KI:SSe^- defect deviate from g_e to a larger extent than for the NaZ lattices and the theoretical calculations predict the same behavior. As in the case of the S_2^- ion, the quantitative agreement with experiment is not that good as for the NaZ lattices. The hyperfine values on the other hand are excellently reproduced. Both for experiment and theory it follows that $A_z > A_y > A_x$, which differs from the situation in the sodium halides.

Since the monovacancy model leads to a good agreement between experiment and theory, we may state that also the larger SSe^- molecular ion replaces a single halide ion in the NaZ and KI lattices.

3. Se_2^- molecular ion

For the NaZ: Se_2^- defects, the same overall agreement is noticed. There are some slight disagreements, e.g., the observed increase in experimental g_x value and decrease in g_z value with increasing halide size. Experimental hyperfine data are available for the NaCl and NaBr lattices and are

TABLE III. A tensor values (MHz) for different diatomic lattice defects doped in NaZ (Z=Cl,Br,I) and KI. All theoretical values correspond with the partial frozen core approximation.

		Experimental SSe^-				Theoretical SSe^-			
		S_2^-	S	Se	Se_2^-	S_2^-	S	Se	Se_2^-
	A_x	$<A_y$[c]	$<A_z$[f]	69[f]	63[d]	−30	−7.5	−95.7	−40.8
NaCl	A_y	108.5	80	432	350	71.3	50.4	293.7	271.9
	A_z	$<A_y$	60	200	287	−10.1	35.7	232.8	234.7
	A_{iso}	n.a.	n.a.	233.6	233.3	10.4	26.2	143.6	155.3
	A_x	n.a.	n.a.	n.a.	60[e]	−31.7	−10.8	−107.6	−46.6
NaBr	A_y	n.a.	n.a.	n.a.	357	71.6	54.1	300	267.3
	A_z	n.a.	n.a.	n.a.	275	−13.8	26.5	173.3	220.5
	A_{iso}	n.a.	n.a.	n.a.	230	8.8	23.3	121.9	147.1
	A_x	n.a.	n.a.	n.a.	n.a.	−32.4	−13.1	−123.6	−44.5
NaI	A_y	n.a.	n.a.	n.a.	n.a.	72.9	57.7	−315.4	257.8
	A_z	n.a.	n.a.	n.a.	n.a.	−15.9	18.7	127.8	239
	A_{iso}	n.a.	n.a.	n.a.	n.a.	8.2	21.1	106.5	105.8
	A_x	$<A_y$[b]	$<A_z$[a]	$<A_z$[a]	$<A_z$[a]	−5.6	4.7	5.6	62.7
KI	A_y	64	$<A_z$	$<A_z$	$<A_z$	37.5	20.8	102.4	24.5
	A_z	93	141	749	740	90.4	123	698.6	732.8
	A_{iso}	n.a.	n.a.	n.a.	n.a.	40.8	49.5	268.9	273.3

[a]Reference 2.
[b]Reference 3.
[c]Reference 4.
[d]Reference 6.
[e]Reference 7.
[f]Reference 8.

relatively well reproduced by the calculations. Theory predicts in all cases $A_y > A_z > A_x$, in agreement with the available experimental data.

The large deviation of the g values from g_e for the KI:Se_2^- defect, is again reproduced by the calculations. The A_z parameter is almost perfectly predicted. In analogy with the SSe^- and S_2^- defects, we may state that the monovacancy model is also valid for the Se_2^- molecular ion.

C. ENDOR parameters

The principal values and tilting angles of the superhyperfine and quadrupole tensors for the considered lattice defects doped in NaCl and NaBr are listed in Tables 4–6. In comparison with our previous study, the quantitative agreement between calculated and experimental anisotropic superhyperfine couplings for interaction 1 (X_2^- molecular ions) and 1′ (XY^- molecular ions), has considerably improved. This is

TABLE IV. A and Q tensor values (MHz) for the Na(1) interaction for different lattice defects doped in NaCl. A_{iso} stands for the isotropic part, while $A_{i,aniso}$ ($i=x,y,z$) represents the anisotropic part of the A tensor. The angles α_A and α_Q are in degrees. All theoretical values correspond with the partial frozen core approximation.

	Experimental SSE^-[a]				Theoretical SSe^-			
	S_2^-[b]	S	Se	Se_2^-[c]	S_2^-	S	Se	Se_2^-
$A_{x,aniso}$	0.57	0.69	1.1	1.69	0.85	0.94	−2.49	−1.96
$A_{y,aniso}$	0	0.11	0.25	0.57	−0.09	0.22	−0.6	−0.87
$A_{z,aniso}$	−0.57	−0.8	−1.35	−2.26	−0.76	−1.18	2.55	2.83
A_{iso}	3.91	3.94	4.96	4.96	−0.29	0.27	−1.58	−1.74
α_A	54.8	24.8	14.6	7.5	25.9	32.4	11.1	10.3
Q_x	−0.53	−0.55	−0.55	−0.56	−0.52	−0.62	−0.64	−0.61
Q_y	0.23	0.24	0.27	0.28	0.21	0.3	0.29	0.31
Q_z	0.3	0.31	0.28	0.28	0.31	0.32	0.35	0.3
α_Q	−35.9	−33.7	−34.8	−33.5	−32.7	−36.6	−33.9	−30.4

[a]Reference 2.
[b]Reference 4.
[c]Reference 7.

TABLE V. A and Q tensor values (MHz) for the Na(2) interaction for different lattice defects doped in NaCl. A_{iso} stands for the isotropic part, while $A_{i,\mathrm{aniso}}$ $(i=x,y,z)$ represents the anisotropic part of the A tensor. The angles β_A and β_Q are in degrees. All theoretical values correspond with the partial frozen core approximation.

	Experimental			Theoretical		
	S_2^-,[b]	SSe^-,[a]	Se_2^-,[c]	S_2^-	SSe^-	Se_2^-
$A_{x,\mathrm{aniso}}$	−0.94	−0.95	−0.91	−1.07	−0.2	−0.99
$A_{y,\mathrm{aniso}}$	0.36	0.15	0.11	0.79	−0.22	0.68
$A_{z,\mathrm{aniso}}$	0.58	0.8	0.8	0.28	0.42	0.31
A_{iso}	−4.41	−4.84	−5.53	−0.02	0.08	−0.08
β_A	0	−24.4	0	0	−44.6	0
Q_x	0.003	0.03	0.05	0.004	0.08	−0.05
Q_y	−0.007	−0.07	−0.09	−0.01	−0.18	0.16
Q_z	0.004	0.05	0.04	0.006	0.1	−0.11
β_Q	0	−21.5	0	0	−0.8	0

[a]Reference 2.
[b]Reference 4.
[c]Reference 7.

confirmed by a better reproduction of the calculated tilting angles of the principal axes. In accordance with the conclusions made in Sec. IV A we do not succeed in giving reasonable estimates for the isotropic superhyperfine values. The partially frozen core as introduced in this work succeeds well in the reproduction of the quadrupole values for both interactions. The calculated tilting angle α_Q is also in excellent agreement with experiment.

The reproduction of superhyperfine and quadrupole parameters for interaction 2 remains problematic. Although the calculated anisotropic values for the X_2^- ions show reasonable agreement with experiment, the results for the SSe^- ion are rather disappointing, especially with respect to the tilting angles β_A and β_Q. It should be noted that in the SSe^- defect the cations 2 are in principle no longer localized in a nodal plane of the unpaired electron wave function and in view of the small values, the DFT results may become extremely dependent on the positions of the cations.

TABLE VI. A and Q tensor values (MHz) for the Na(1) and Na(2) interaction for Se_2^- doped in NaBr (Ref. 7). A_{iso} stands for the isotropic part, while $A_{i,\mathrm{aniso}}$ $(i=x,y,z)$ represents the anisotropic part of the A tensor. The angles α_A and α_Q are in degrees. All theoretical values correspond with the partial frozen core approximation.

	Experimental		Theoretical	
	Na(1)	Na(2)	Na(1)	Na(2)
$A_{x,\mathrm{aniso}}$	1.36	−0.75	−1.51	−0.76
$A_{y,\mathrm{aniso}}$	0.63	0.26	−0.95	0.71
$A_{z,\mathrm{aniso}}$	−1.99	0.49	2.46	0.05
A_{iso}	4.39	−4.77	−1.33	−0.05
α_A	7.7	0	14.4	0
Q_x	−0.46	n.a.	−0.43	−0.08
Q_y	0.2	n.a.	0.22	0.18
Q_z	0.25	n.a.	0.21	−0.1
α_Q	−32.9	n.a.	−28.7	0

D. Comments on the signs of the superhyperfine and quadrupole parameters

We notice some striking discrepancies between the experimental and theoretical signs of the (super)hyperfine and quadrupole parameters, even though the absolute values agree quite well. One can wonder in how far all experimental signs are really correct. First, we like to emphasize that the signs carry additional information about the electronic and geometric structure of the paramagnetic defect and its lattice surroundings. But even though these signs are difficult to assess experimentally, they can often be ''guessed'' by using additional information or by considering trends in comparable systems. Hence the experimental ''prediction'' of the signs can be the subject of some discrepancies with theory. The most striking discrepancy in signs is observed in Table 5. The quadrupole tensor of the Na(2) interaction for Se_2^- in NaCl gives opposite signs. A sign reversal would lead to a reasonable agreement. On the contrary, if we look at the comparable quantities for the Na(1) interaction in Table 4, there is obviously no need for a sign reversal. For the superhyperfine interaction with Na(1) nuclei neighboring Se, however, the discrepancy between the experimental and theoretical signs for SSe^- and Se_2^- is quite general. At this stage the reasons for these observed discrepancies are not yet known and further study on these items is in progress.

E. Comments on the isotropic couplings

The present study shows that the quantitative reproduction of isotropic hyperfine coupling constants poses still serious problems. Isotropic couplings arise due to the appearance of spin density at the position of the nucleus. This contact hyperfine interaction is greatly amplified by core polarization of the s-electrons and is mediated by attractive exchange interactions between spin orbitals with parallel spins in successive core shells. A relaxation of the frozen core approximation would be expected to enlarge the core polarization, but the results do not reveal much improvement suggesting an inadequacy of the used DFT functional for this type of calculations.[35] Indeed, the exact exchange interaction which is strongly non-local and which is responsible for an adequate core polarization is replaced by a local spin density approximation. The insufficient core polarization in the present results is an inherent consequence of the specific intrinsic nature of the employed density functional, and underlines the limits of DFT methods in the reproduction of some spin dependent properties.

V. CONCLUSION

In this work we presented an extended version of the model outlined in Ref. 1. The extension mainly consists in a

partial unfreezing of the 88-atom cluster. It was found that important shortcomings of the previous model using the frozen core approximation are now removed. In particular, the quadrupole tensors of the alkali neighbors in the g_x-g_z plane are now reproduced in a very satisfactory way.

For those quantities whose theoretical prediction was satisfactory even with the full frozen core approximation, it turns out that the unfreezing effect of the core has little effect, in this way keeping the good experimental agreement and even slightly improving it. In this context, we underline the excellent reproduction of the g values for all considered diatomic defects. All ground states were correctly predicted using the same procedure and level of theory for all defects and lattices. All results give evidence for the validation of the monovacancy model for the SSe^- and Se_2^- molecular ions.

In general, the chalcogen hyperfine tensors show good agreement with experiment. In some cases discrepancies are noticed when comparing experimental and theoretical hyperfine values. These are mainly due to difficulties in reproducing the correct isotropic coupling values.

Finally, the agreement between experimental and theoretical quadrupole values and orientations of principal axes is nearly perfect. The frozen core approximation appears not to be suitable for an accurate calculation of quadrupole tensors, although prediction of qualitative trends is perfectly possible within this approximation. The reproduction of superhyperfine tensors remains somewhat problematic. As a general conclusion, we have found that *ab initio* cluster *in vacuo* calculations using DFT methods succeed in reproducing EPR and ENDOR experimental data of diatomic paramagnetic defects doped into alkali halide lattices in an overall very satisfactory way.

ACKNOWLEDGMENT

The authors would like to thank the Fund for Scientific Research (FWO-Flanders, Belgium) for financial support.

*Corresponding author. Email address: freddy.callens@rug.ac.be

[1] F. Stevens, H. Vrielinck, F. Callens, E. Pauwels, and M. Waroquier, Phys. Rev. B **66**, 134103 (2002).
[2] L. E. Vannotti and J. R. Morton, Phys. Lett. **24A**, 250 (1967).
[3] L. E. Vannotti and J. R. Morton, Phys. Rev. **161**, 282 (1967).
[4] P. Matthys, F. Callens, and E. Boesman, Solid State Commun. **45**, 1 (1983).
[5] F. Maes, F. Callens, P. Matthys, and E. Boesman, Phys. Status Solidi B **161**, K1 (1990).
[6] F. Maes, F. Callens, P. Matthys, and E. Boesman, J. Phys. Chem. Solids **51**, 1289 (1990).
[7] F. Maes, P. Matthys, F. Callens, and E. Boesman, Solid State Commun. **80**, 583 (1991).
[8] F. Maes, S. Van Doorslaer, F. Callens, P. Moens, P. Matthys, and E. Boesman, J. Phys.: Condens. Matter **6**, 8065 (1994).
[9] S. Van Doorslaer, F. Maes, F. Callens, P. Matthys, and E. Boesman, J. Chem. Soc., Faraday Trans. **92**, 1579 (1996).
[10] S. Van Doorslaer, F. Callens, F. Maes, P. Matthys, and E. Boesman, Phys. Rev. B **54**, 1145 (1996).
[11] S. L. Altman and P. Herzig, *Point-Group Theory Tables* (Clarendon Press, Oxford, 1994).
[12] A. Abragam and B. Bleaney, *Electron Paramagnetic Resonance of Transition Ion* (Clarendon Press, Oxford, 1970).
[13] W. Känzig and M. H. Cohen, Phys. Rev. Lett. **3**, 509 (1959).
[14] R. Zeller and W. Känzig, Helv. Phys. Acta **40**, 845 (1967).
[15] R. T. Shuey and H. R. Zeller, Helv. Phys. Acta **40**, 873 (1967).
[16] R. G. Parr and W. Yang, *Density Functional Theory of Atoms and Molecules* (Oxford University Press, Oxford, 1989).
[17] T. Ziegler, Chem. Rev. **91**, 651 (1991).
[18] D. R. Salahub, M. Castro, and E. Y. Proynov, in *Relativistic and Electron Correlation Effects in Molecules and Solids*, edited by G. L. Malli (Plenum, New York, 1994).
[19] ADF, http://tc.chem.vu.nl/SCM., Department of Theoretical Chemistry, Vrije Universiteit Amsterdam.
[20] E. J. Baerends, D. E. Ellis, and P. Ros, Chem. Phys. **2**, 41 (1973).
[21] F. Guerra, O. Visser, J. G. Snijders, G. te Velde, and E. J. Baerends, in *Methods and Techniques in Computational Chemistry METECC-95*, edited by E. Clementi and G. Corongiu (STEF, Cagliari, 1995), pp. 305–395.
[22] E. van Lenthe, P. Wormer, and A. van der Avoird, J. Chem. Phys. **107**, 2488 (1997).
[23] E. van Lenthe, A. van der Avoird, and P. Wormer, J. Chem. Phys. **108**, 4783 (1997).
[24] E. van Lenthe and E. J. Baerends, J. Chem. Phys. **112**, 8279 (2000).
[25] All standard ADF basis sets are available on the net at http://www.scm.com/Doc/atomidata.
[26] S. H. Vosko, L. Wilk, and M. Nusair, Can. J. Phys. **58**, 1200 (1980).
[27] C. Chang, M. Pelissier, and P. Durand, Phys. Scr. **34**, 394 (1988).
[28] J.-L. Heully, I. Lindgren, E. Lindroth, S. Lundqvist, and A. M. Martensson-Pendrill, J. Phys. B **101**, 1272 (1994).
[29] E. van Lenthe, E. J. Baerends, and J. G. Snijders, J. Chem. Phys. **99**, 4597 (1993).
[30] E. van Lenthe, E. J. Baerends, and J. G. Snijders, J. Chem. Phys. **101**, 9783 (1994).
[31] E. van Lenthe, J. G. Snijders, and E. J. Baerends, J. Chem. Phys. **105**, 6505 (1996).
[32] E. van Lenthe, R. V. Leeuwen, E. J. Baerends, and J. G. Snijders, Int. J. Quantum Chem. **57**, 281 (1996).
[33] E. van Lenthe, A. E. Ehlers, and E. J. Baerends, J. Chem. Phys. **110**, 8943 (1999).
[34] F. Herman and F. Skilman, *Atomic Structure Calculations* (Prentice-Hall, Engelwood Cliffs, NJ, 1963).
[35] M.L. Munzarová, P. Kubáček, and M. Kaupp, J. Am. Chem. Soc. **122**, 11 900 (2000).